[Frontiers in Bioscience 9, 2045-2055, September 1, 2004]

BUILDING A FUNCTIONAL ARTERY: ISSUES FROM THE PERSPECTIVE OF MECHANICS

Rudolph L. Gleason, Jin-Jia Hu and Jay D. Humphrey

Department of Biomedical Engineering and M.E. DeBakey Institute, Texas A&M University, College Station, TX 77843-3120, USA

TABLE OF CONTENTS

1. ABSTRACT

Despite the many successes of arterial tissue engineering, clinically viable implants may be a decade or more away. Fortunately, there is much more that we can learn from native vessels with regard to designing for optimal structure, function, and properties. Herein, we examine recent observations in vascular biology from the perspective of nonlinear mechanics. Moreover, we use a constrained mixture model to study potential contributions of individual wall constituents. In both cases, the unique biological and mechanical roles of elastin come to the forefront, especially its role in generating and modulating residual stress within the wall, which appears to be key to multiple growth and remodeling responses.

2. INTRODUCTION

There have been many remarkable achievements in the field of arterial tissue engineering since publication of the landmark paper by Weinberg and Bell (1). For example, in contrast to early tissue-engineered arteries, recent successes include constructs that have an intact endothelium, a layered wall that resembles the intima, media and adventitia, burst pressures up to 2000 mmHg, smooth muscle contractility, and short term patency in animal trials (e.g., (2-4)). Nevertheless, when asked how long it will be until tissue-engineered arteries are available for implantation in humans, many leading experts suggest that clinical success may be at least a decade away.

It is unlikely that a tissue-engineered artery will mimic exactly a native vessel, thus we must identify those aspects of the native histology, biology, and mechanics that are essential to the long-term success of an implanted construct. Ku and Han (5) suggest five basic design criteria: "(a) high mechanical strength, (b) a lumen composed of living cells performing specific biological functions, (c) short- and long-term functional adaptive responses to varying hemodynamic conditions, (d) low thrombogenicity, and (e) very low immunoreactivity or host versus graft response." Early on, "high mechanical strength" typically implied a high burst pressure and adequate suture retention. Although these criteria were not fulfilled by early constructs, multiple techniques have proven effective in remedying this situation: e.g., cellular compaction of collagen matrices on mandrels, culturing constructs in media that includes ascorbic acid, select amino acids and copper, and subjecting developing constructs to cyclic strains. Recently, it has been suggested further that there may also be a need to mimic better the full pseudoelastic or viscoelastic properties of a native artery (e.g., (2, 4)), particularly to minimize adverse mechanobiological responses by the host vessel. For example, minimizing "compliance mismatch" between a construct and host may decrease neointimal hyperplasia by the host near the anastomosis. Indeed, it may also be necessary to mimic well the native biomechanical properties and stress fields in order for a construct to be capable of adaptive, rather than maladaptive, short- and long-term remodeling.

The goal of this paper is to review aspects of the

biomechanics of normal arteries that appear to endow these vessels with their remarkable ability to adapt well to altered mechanical loads, including pressures, flows, and axial forces. In particular, whereas much of the attention in tissue engineering appears to have focused on collagen, we address aspects of the contribution of elastin to the biomechanics of the wall that appear to be critical to the properties of and stresses within the native artery. For example, elastin appears to play a key role in the development of residual stresses, which in turn appear to be vital to normal arterial physiology. This observation suggests that it may be helpful to engineer residual stresses into thick-walled functional constructs, which in turn may require a specific deposition of elastin.

3. BACKGROUND

3.1. Material Behavior

A constitutive relation describes responses of a material to applied loads under conditions of interest and thereby can provide a concise representation of material behavior. Many frameworks have been used to describe the mechanical behavior of normal arteries – including linearized elasticity, incremental elasticity, pseudoelasticity, viscoelasticity, and poroelasticity – but it is now clear that, at a minimum, the geometric and material nonlinearities must be included (6). Although there is no well-accepted nonlinear descriptor of the constitutive behavior of arteries (see (7)), multiple relations provide reasonable estimates for cyclic, physiologic loads. One such relation combines that proposed by Chuong and Fung (8) for passive behavior [1] with that proposed by Rachev and Hayashi (9) for active behavior. It is,

$$\mathbf{t} = -p\mathbf{I} + \frac{1}{2}ce^{Q}\mathbf{F}\cdot\frac{\partial Q}{\partial \mathbf{E}}\cdot\mathbf{F}^{T} + T_o(Ca^{2+})\lambda_\theta\left[1-\left(\frac{\lambda_M-\lambda_\theta}{\lambda_M-\lambda_o}\right)^2\right]\mathbf{e}_\theta\otimes\mathbf{e}_\theta \quad (1)$$

where $\mathbf{t}$ is the Cauchy (true) stress, p a Lagrange multiplier that enforces incompressibility during transient loading, $\mathbf{I}$ the identity tensor, $\mathbf{F}$ the deformation gradient, $\mathbf{E} = (\mathbf{F}^T\cdot\mathbf{F} - \mathbf{I})/2$ the Green strain, $T_o(Ca^{2+})$ an activation function for the smooth muscle (values of which typically range from 0 to 100 kPa), λ_M and λ_o are values of the circumferential stretch λ_θ at which vascular smooth muscle activation is maximum or zero, respectively, and

$$Q = c_1E_{RR}^2 + c_2E_{\Theta\Theta}^2 + c_3E_{ZZ}^2 + 2c_4E_{RR}E_{\Theta\Theta} + 2c_5E_{\Theta\Theta}E_{ZZ} + 2c_6E_{ZZ}E_{RR} \quad (2)$$

where E_{AB} are physical components of $\mathbf{E}$ relative to (R, Θ, Z), the radial, circumferential, and axial directions in a passive reference configuration; c and c_j (j = 1, 2, …, 6) are material parameters for the passive response. Albeit not perfect, this relation captures salient general characteristics of a native artery: nonlinear, nearly elastic, anisotropic, active-passive, and nearly incompressible behavior over finite strains (see Figure 7.32 in (6)). Moreover, equations 1-2 capture the unique behavior whereby cyclic pressurization does not alter the axial force when the artery is at an *in vivo* axial length (see Figures 7.20-21 in (6)). This equation is thus useful for estimating overall transmural stress fields.

3.2. Native Stress Fields

Recent findings that vascular cells (endothelial, smooth muscle, and fibroblasts) are sensitive to changes in their mechanical environment emphasize the need to predict well the transmural distributions of stress and strain. Inertial effects are often negligible (10), thus we shall consider a simple quasi-static simulation. First, however, note that one of the most important discoveries in arterial mechanics is that excised, intact, unloaded segments are not stress-free. Rather, arteries are residually stressed, which is to say that stresses remain in the absence of applied tractions. Notwithstanding yet unknown complexities of the residual stress field, consider the simple method of Chuong and Fung (8) to account for residual stress within the context of a finite extension and inflation. Let the deformation gradient be given by

$$\mathbf{F} = \mathrm{diag}\left[\frac{\partial r}{\partial R}, \frac{r\pi}{R\Theta_o}, \lambda\Lambda\right], \quad (3)$$

where (r, θ, z) denotes the current location of a material particle with reference location (R, Θ, Z) in an unloaded, radially-cut configuration; Θ_o and Λ denote the residual stress related opening angle and axial stretch (i.e., an excised arterial ring will 'spring open' when cut radially for this relieves at least part of the residual stress) whereas λ denotes an additional load-induced axial stretch. Figure 1 shows computed transmural stresses in the presence or absence of residual stress and smooth muscle activation, which appear to work synergistically to homogenize the stress field despite strong geometric and material nonlinearities [2]. Indeed, out of this complex boundary value problem arises a simple stress field, one that seems reasonable teleologically for it would allow smooth muscle cells to function within a similar (homeostatic) mechanical environment independent of location within the wall. It is easy to imagine that such a uniform stress field could be a target for normal development as well as subsequent growth and remodeling (G&R). A critical question for tissue engineering, therefore, is: How do residual stresses develop in arteries? To this end, let us consider some observations from the literature.

4. LESSONS FROM ARTERIAL GROWTH AND REMODELING

4.1. Development

It is purported that Aristotle (384-322 B.C.) said, "Here and elsewhere we shall not obtain the best insight into things until we actually see them growing from the beginning." Indeed, if an 'optimal' homeostatic state of stress (or strain) exists, which we assume, then we must try to learn from normal arterial development how this state is achieved via a complex layered composition that forms via a sequence of additions and removals.

Whether via vasculogenesis or angiogenesis, arteries begin as a small tube of endothelial cells that lay down a basement membrane initially consisting largely of fibronectin, but later laminin, type IV collagen, and select

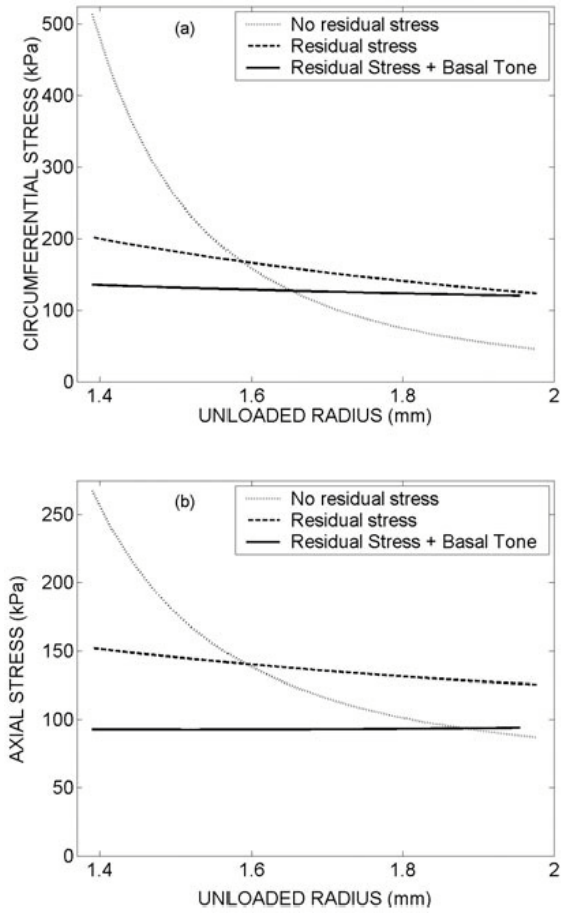

Figure 1. Computed transmural circumferential (a) and axial (b) stresses for three cases: passive with and without residual stress and basal tone with residual stress. Note that the residual stress (i.e. elastin) plays a key role in homogenizing the stress field.

proteoglycans (note: fibronectin may promote migration and proliferation whereas laminin may promote cell adhesion and differentiation and type IV collagen may promote cell adhesion, cell spreading, and cell survival (11-12)). The endothelial cells align in the direction of the blood flow (and perpendicular to the direction of cyclic stretch) and, as development proceeds, it appears that signals from this monolayer of endothelial cells recruit smooth muscle precursor cells that align primarily in the direction of the cyclic circumferential stretch. These smooth muscle cells begin to synthesize and organize an extracellular matrix (eventually consisting largely of insoluble elastin and select collagens as well as various proteoglycans), and they either proliferate or recruit additional smooth muscle cells as the hemodynamic loading increases. Finally, a fibroblast-populated, collagen-rich outer layer forms as the adventitia, and the smooth muscle cells of the media differentiate from a synthetic to a quiescent, contractile phenotype. This sequential addition of material results in a wall that thickens as the blood pressure increases, which appears to maintain the mean circumferential wall stress near an 'optimal' value (13); similarly, the lumen enlarges as the blood flow increases, which appears to maintain the mean wall shear stress near an 'optimal' value (14). As noted above, it is out of this genetically and epigenetically regulated, complex, layered structure that an apparently nearly uniform homeostatic stress field arises.

The mechanical behavior exhibited by a material arises, of course, from its internal constitution, which includes the distributions, orientations, and interconnections of its constituents. Elastin is much less stiff than the fibrillar collagens, but much more stable biologically and thermally. In addition, elastin is perhaps the most "elastic" biological protein; it exhibits a nearly linear stress-stretch response, with little hysteresis, over large extensions. Since the classic paper by Roach and Burton (15), it has been thought that elastin contributes to the entire pressure-distension curve of an artery whereas the collagen, which appears undulated in the unloaded configuration, contributes primarily at higher pressures; it is also now well accepted that, in general, elastin gives an artery its elasticity, collagen resists tensile forces, glycosaminoglycans (GAG) resist compressive forces, and smooth muscle cells endow the artery with its innate ability to regulate its diameter (16). Nevertheless, enzymatic degradation of elastin can result in a marked dilatation of an artery whereas degradation of collagen can result in leakage or rupture; the former is thought to be related to the development of aneurysms (e.g., (17)).

In addition to its basic structural role (e.g., elastic recoil), we now know that elastin also plays a key role in the regulation of residual stress in arteries. Greenwald *et al.* (18) showed in large arteries containing significant elastin (e.g., thoracic aorta) that treatment with elastase significantly reduced the opening angle ($\Phi_o \equiv \pi - \Theta_o$) whereas treatment with collagenase had little effect. They concluded that "residual strains are largely due to the elastic component of the vessel wall." Despite some differences in findings, results of Zeller and Skalak (19) support this conclusion. They wrote, "collagen fibers contribute an increasing proportion of structural integrity from the inner (intimal) to outer (adventitial) wall" but "the presence of elastin throughout the entire wall is responsible for maintaining the zero-stress configuration." In other words, arterial elastin appears overall to be in tension in an intact, unloaded configuration, which appears to contribute to the collagen being highly undulated, perhaps compressed, in this configuration. Because of the strong material and geometric nonlinearities, resulting small residual stresses (~3 kPa) can reduce tremendously the possible gradients in stress (cf. Figure 1).

We conclude, therefore, that if the early development and long-term stability of elastin is essential in maintaining residual stresses, and if residual stresses are fundamental to a uniform homeostatic stress (or strain) field in the wall that optimizes the mechanobiology, then there is a need to discover how the deposition of elastin generates the residual stress. Returning to arterial development, Davis (11) suggests that the elastic lamina in the aorta are formed "completely" prior to maturation even though the vessel subsequently enlarges another 25%. If

this is the case, the elastic fibers will be stretched in maturity to a degree that they could remain stretched even when the artery is unloaded; moreover, given their exceptional biological stability and elasticity, these initially stretched fibers could remain stretched for long periods, perhaps to the beginning of aging. Hence, albeit a highly compliant material that was long thought to dominate only the low-pressure behavior, the mechanical advantage of appropriately deposited elastin may be far reaching. Moreover, with regard to deposition and organization of constituents, we see that 'sequence matters.'

Finally, recent observations reveal that elastin plays equally vital biological roles. For example, insoluble elastin appears to promote the contractile phenotype of neighboring smooth muscle, which is to say to reduce migratory, proliferative, and synthetic activity (20). Indeed, elastin-knockout mouse models reveal an increased cellularity in the sub-endothelial space and a concomitant narrowing of the vessel (21). That is, the absence of an internal elastic lamina appears to allow postnatal migration into and accumulation of smooth muscle cells within the sub-intima "in systemic and pulmonary arteries of all sizes." This finding is likely related to the neointimal accumulation of synthetic cells in maturity wherein the inner layers of elastin are damaged by balloon injury, inflammation, or thrombosis (22). This growth inhibitory role of insoluble elastin is very different from that of tropoelastin (i.e., the soluble precursor), which appears to be chemotactic for smooth muscle (20). There appears, therefore, to be a carefully coordinated sequence through which cells migrate and proliferate early on and adhere and differentiate later on, which is controlled in part by a tightly regulated deposition, organization, and subsequent cross-linking of elastin. Indeed, nitric oxide and endothelin-1, which are regulated (in part) by mechanical loading, have also been identified in the coordination of tropoelastin production and cross-linking via the production of lysyl oxidase (23-24). Multiple microfibrillar proteins (e.g., fibulin and fibrillin-2) appear to serve as a scaffold for tropoelastin and thereby contribute to this sequential organization. It is interesting that tropoelastin is produced in maturity in various vascular diseases, yet it does not appear to cross-link effectively and thus remains biologically as well as mechanically compromised (25). It is also interesting to note that in comparison to wildtype ($ELN^{+/+}$) mice, a hemizygous mouse model ($ELN^{+/-}$) of decreased (~35-50%) elastin production develops a higher blood pressure during development. According to Dietz and Mecham (22), "Wall stress in the $ELN^{+/-}$ artery is different because the elastin content is lower. Because $ELN^{+/-}$ SMC cannot make more elastin, they compensate by organizing more cell layers." Whereas adding more cell layers is a possible adaptive response during development, this appears to be less possible in maturity. Hence, the compensatory attempt must focus on adding material within extant layers, either smooth muscle or collagen (see, for example, (26)).

4.2. Adaptation in Maturity

Fung (27) suggested that "one of the best ways to study tissue engineering is to investigate the changes that can occur in normal organs when the stress and strain fields are disturbed from the normal homeostatic condition." In general, arteries tend to increase (decrease) their lumen in response to a sustained increase (decrease) in blood flow and they tend to thicken (thin) their wall in response to a sustained increase (decrease) in blood pressure. Hence, just as development appears to proceed towards an optimal biomechanical state, so too do many responses to altered loads. Indeed, recall that Ku and Han (5) list short- and long-term functional adaptations to hemodynamic conditions among their five criteria for tissue-engineered vessels. Because these changes correlate well with restorations in stress towards original values, note that representative values of the mean wall shear stress and circumferential stress in large arteries are, respectively,

$$\tau_w = \frac{4\mu Q}{\pi a^3} \approx 1.5 \text{ Pa}\ ,\ \sigma_\theta = \frac{Pa}{h} \approx 150 \text{ kPa}\ , \qquad (4)$$

where μ is the fluid viscosity, Q the mean volumetric flow-rate, a the deformed inner radius, P the mean transmural pressure, and h the deformed wall thickness ($h = b - a$, where b is the deformed outer radius). It is reasonable to expect, of course, that arteries simultaneously seek to maintain all stresses near homeostatic values at all times (28-29), not just individual components in special cases. Thus, the mean axial stress σ_z may similarly be regulated via G&R mechanisms, where

$$\sigma_z = \frac{f_z}{\pi(b^2 - a^2)} = \frac{f_z}{\pi h(2a + h)} \approx 100 \text{ kPa} \qquad (5)$$

and f_z is the axial load.

We submit that in response to altered loading (whether it be flow, pressure, axial load, or combinations thereof), the vessel typically experiences an immediate 'passive' elastic response (e.g., distension in response to increased pressure), a subsequent short-term adaptation via a vasoactive control of the lumen (which occurs in minutes to hours and seeks to restore τ_w toward normal values) that may result in a new 'vasoaltered' configuration, and if the altered mechanical loading persists, a long-term adaptation involving turnover (i.e., coordinated production and removal) of cells and extracellular matrix in the vasoaltered configuration and/or remodeling of extant constituents (e.g., changes in the distributions, interconnections, and reference lengths). This long-term response occurs over days to weeks (30). It seems, however, that arterial G&R proceeds differently in maturity than in development. Examples include the much higher rates of adaptation in developing arteries (with higher turnover of cells and matrix) and an absent or ineffective elastogenesis in maturity. With these ideas in mind, let us consider observations from the literature on flow-, pressure-, and axial stretch-induced G&R.

4.3. Flow-induced G&R

Let the altered volumetric flow rate $Q = \varepsilon Q_h$, where Q_h is the homeostatic rate prior to flow alteration and ε is a parameter. Equation $(4)_1$ reveals that *if* τ_w is to be restored, *then* the luminal radius $a(s) \to \varepsilon^{1/3} a(0)$, where

s is the G&R time, with $s = 0$ denoting the homeostatic state prior to a step change in loading. If this step change in flow is sustained and the alteration in a is achieved fully via a single vasoactive response, then its value should remain unchanged during G&R. In this case, equation $(4)_2$ reveals further that, *if* the pressure remains constant and *if* the circumferential stress is restored to its homeostatic value during G&R, *then* the wall thickness $h(s)$ must tend to $\varepsilon^{1/3}h(0)$. Such thickening or thinning in response to an increase ($\varepsilon > 1$) or decrease ($\varepsilon < 1$) in flow would be accomplished primarily via the production or removal of material, respectively. Finally, equation (5) reveals that if axial stress is also restored to its homeostatic value, then the axial load f_z should tend to $\varepsilon^{2/3} f_z(0)$.

Kamiya and Togawa (31) showed that equation $(4)_1$ is satisfied (i.e., $a(s) \to \varepsilon^{1/3} a(0)$) in canine carotid arteries at 6-months given an increased flow wherein $\varepsilon <$ 3.5, but not for $\varepsilon = 4.0$ to 8.5. Many later reports support the finding that wall shear stress is often restored close to homeostatic values following a sustained alteration in flow. Results from the literature are less clear whether the mean circumferential stress is likewise restored (i.e., that wall thickness $h(s) \to \varepsilon^{1/3} h(0)$). For example, Zarins *et al*. (32) reported that after 6-months of an increased flow in the iliac artery of an adult monkey, $\varepsilon =$ 9.6 (thus $\varepsilon^{1/3} = 2.1$) and $a = 2.1a(0)$, but based on their data (and assuming no changes in axial length) $h =$ $1.3h(0)$. Thus, the radius remodeled as predicted by equation $(4)_1$ while wall thickness did not reach the optimal value in 6 months predicted by $(4)_2$. Similar reports hold for adult and immature animals. Nevertheless, a few studies show $h(s) \to \varepsilon^{1/3} h(0)$, as, for example, (33-34). Finally, with regard to the evolution in residual stress in flow-induced G&R, Lu *et al*. (35) showed that the opening angle Φ_o significantly decreased over weeks in flow-loaded rat femoral arteries (ε from 3.0-3.8) compared to control groups (i.e., Φ_o ~110° to ~80° at 8 and 12 weeks).

4.4. Hypertension

In response to a step change in pressure, $P = \beta P_h$, where P_h is the initial 'homeostatic' pressure and β is a parameter, the immediate passive response of the artery is to distend (or retract), thereby altering the inner radius and wall shear stress. In response to the altered τ_w, a subsequent active response appears to adjust the lumen both directly (myogenic response) and indirectly (via endothelial release of vasoactive molecules). If the lumen is restored, equation $(4)_2$ requires that h(s) must tend to $\beta\, h(0)$ for the circumferential wall stress to be restored to its homeostatic value and equation (5) requires that f_z must tend toward $\left[\beta(2a_o + \beta h_o)/(2a_o + h_o)\right] f_z(0)$ to restore the axial stress.

Fung and Liu (36) report excellent data on the time-course of changes in wall stress and the residual stress related opening angle in an aortic-coarctation rat model. Following immediate changes due to vessel distension and possible baroreceptor response, acute changes likely include vasoconstriction. They proposed that the wall then thickened due to G&R such that the unloaded thickness to radius ratio, H:$A \propto \hat{A} + \hat{B}(1 - e^{-cs})$, where $\hat{A}$, $\hat{B}$, and c are constants and s is G&R time. They similarly found that the opening angle tended to return exponentially towards baseline at 20-40 days following an early increase that peaked at ~5 days. The initial increase in Φ_o suggests that the inner wall adapted first.

4.5. Axial Stretch-induced G&R

In response to a step change in axial length $\ell(s) = \delta \ell(0)$, where $\ell(0)$ is the *in vivo*, homeostatic length of the vessel, and δ is a parameter, the vessel will initially narrow and thin. Again, a vasoactive response could promote $a(s) \to a(0)$ and G&R could restore $h(s)$ toward $h(0)$. In an *in vivo* model wherein the left common carotid artery in the rabbit was subjected to an ~22% increase in axial extension while maintaining blood flow and blood pressure at near normal values, Jackson *et al*. (37) showed that the axial strain [defined as (*in situ* length – *in vitro* length)/(*in vitro* length)] decreased from 97 ± 2% to 72 ± 1% at 3 days, 67 ± % at 7 days, and 55 ± 3% at 35 days, with ~50% being a normal value. Thus, the artery remodeled rapidly in such a way that the axial strain (or stress) tended to re-normalize. They reported that this G&R was due to dramatically increased rates of cellular proliferation (particularly at 3 days), and "unprecedented" increases in the synthesis of elastin and collagen, with cellular apoptosis and the upregulation of matrix metalloproteinases (e.g., MMP-2 and MMP-9) playing significant roles. Finally, based on hemodynamic measurements and morphologic examinations of pressure-fixed cross-sections, they concluded, "changes in neither circumferential tensile stress nor shear stress can account for the rapid remodeling that normalized increases in axial strain." Similar findings have been reported by Han *et al*. (38) and Clerin *et al*. (39) who demonstrated significant remodeling of porcine carotid arteries in response to increases in axial stretch, albeit in an *ex vivo* setting.

4.6. Growth and Remodeling Biomechanics

Mathematical models allow one to contrast possible consequences of competing hypotheses, to perform parametric studies to identify dominant effects, and to integrate diverse observations into a common theoretical framework. Most models of arterial G&R are based on the concept of kinematic growth (see (40)). Briefly, growth is described via evolution relations that track deformations between two fictitious stress-free configurations: an original body is fictitiously cut into small stress-free pieces, each of which is allowed to grow separately into larger stress-free pieces. Because the growth of each piece need not be compatible, internal forces are typically needed to reassemble the grown pieces into a contiguous configuration, which produces residual stress. Elastic deformations are then referenced to the intact, residually-stressed configuration.

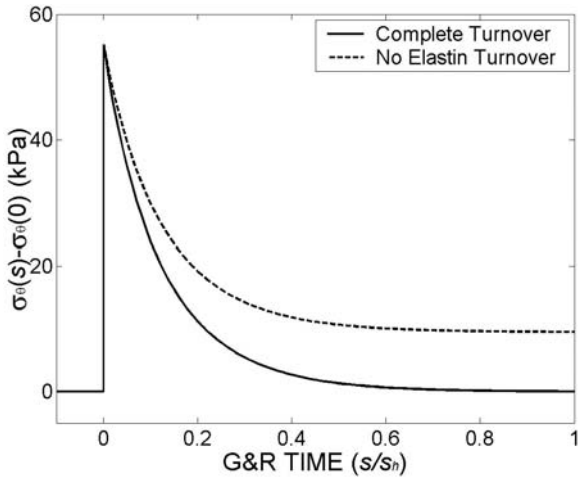

Figure 2. Evolution of the difference between the current circumferential stress $\sigma_\theta(s)$ and its original homeostatic value $\sigma_\theta(0)$ for an abrupt, 50% increase in flow. Notice that complete turnover of all three constituents at their homeostatic stretch (solid line) allows full recovery of $\sigma_\theta(0)$, whereas the absence of elastin turnover yields a sub-optimal adaptation given all other prescribed conditions.

We recently proposed a fundamentally different approach, one that accounts for the separate material behaviors and rates of production and removal of individual constituents within the context of a constrained mixture (41). The basic equation for the stress response, at any G&R time *s*, is written in terms of the true density production of constituent *k*, the survival time of constituent *k* (i.e., material will contribute to the load carrying capability only as long as it remains), and $\mathbf{f}^k(\ldots)$ the stress response function for constituent *k*, which depends on the deformation experienced by that constituent relative to its individual natural configuration; equilibrium in the absence of body forces is enforced in terms of the total (mixture) stress via $\nabla \cdot \mathbf{t} = \mathbf{0}$. For more details, see the original paper. Note, however, that this formulation emphasizes the importance of the history of the turnover of the individual constituents and the possible evolution of their natural configurations (i.e., each configuration in which $\mathbf{f}^k(\ldots) = \mathbf{0}$, not $\mathbf{t} = \mathbf{0}$). This equation recovers the simple rule-of-mixtures relation when the deformation and natural configurations do not evolve following a single perturbation in loading.

For purposes of illustration, let us consider only mean values of wall stress, with a wall that consists of three structurally significant constituents (elastin, collagen, and smooth muscle) that are allowed to turnover in but a single, altered configuration (cf. (42)). For a finite inflation and extension, the components of the individual 2-D deformation gradients are

$$\lambda_\theta^k = \frac{a^k}{A^k} \equiv \frac{a}{A^k}\,,\ \lambda_z^k = \frac{\ell^k}{L^k} \equiv \frac{\ell}{L^k}\,, \qquad (6)$$

and mean values (σ_i^k with $i = \theta$ or z) of the individual Cauchy stress are given constitutively by

$$\sigma_\theta^k = \hat{\sigma}_\theta^k(\lambda_\theta^k, \lambda_z^k)\,,\ \sigma_z^k = \hat{\sigma}_z^k(\lambda_\theta^k, \lambda_z^k)\,. \qquad (7)$$

Here, *a* and ℓ are the inner radius and axial length of the artery in the current configuration and *A* and *L* are similar quantities in an original unloaded configuration; the superscript *k* denotes both an individual constituent and its natural configuration. Assuming a constrained mixture, the individual constituents deform with particles of the single continua (i.e., $a^k \equiv a$ and $\ell^k \equiv \ell$). Assuming a rule-of-mixtures relation for the stress response at any G&R time *s*, with $\phi^k(s)$ denoting the mass fraction of constituent *k*, equilibrium requires [3] (42)

$$\sigma_\theta = \frac{Pa}{h} = \sum \phi^k(s)\hat{\sigma}_\theta^k\left(\frac{a(s)}{A^k(s_p)}, \frac{\ell(s)}{L^k(s_p)}\right), \qquad (8)$$

$$\sigma_z = \frac{f}{\pi h(2a+h)} = \sum \phi^k(s)\hat{\sigma}_z^k\left(\frac{a(s)}{A^k(s_p)}, \frac{\ell(s)}{L^k(s_p)}\right), \qquad (9)$$

wherein the natural configurations (A^k *and* L^k) are allowed to evolve separately, with s_p denoting the particular time at which a constituent was produced. For example, cells and select ECM proteins (e.g., collagen) turnover regularly and may acquire new natural configurations whereas other ECM proteins (e.g., elastin) turnover slowly and thus can retain the natural configuration at which they were produced in development.

We have used this framework to simulate the evolution of wall stresses and geometry in response to a sustained step change in luminal flow for a model artery in which all three the primary structural constituents turnover completely and are laid down at a 'homeostatic' value of stretch (Case 1). These results are compared to those wherein elastin turnover is negligible (Case 2). See (42) for details. Notice that the stress (plotted as the difference between the current and initial values) is restored to initial values in Case 1 but not necessarily in Case 2 (Figure 2). Indeed, in the latter case we find that the geometric changes (e.g., thickening) are 'sub-optimal' similar to many reports in the literature on mature vessels. Again, therefore, the effect of the compliant elastin appears to be far reaching.

5. TISSUE-ENGINEERED VESSELS

We have identified several biomechanical characteristics exhibited by native arteries – including a nonlinear pseudoelastic behavior, a homogenized stress field that results from residual stresses and smooth muscle activation, a constant axial load during inflation at the *in vivo* length**,** material nonuniformity (with different constituents contributing important characteristics to the overall behavior), and an ability to adapt structurally, geometrically, and materially in response to altered loads. The question remains, 'which characteristics must we build into a tissue-engineered artery?' Here, let us consider this question with the aid of our constrained mixture model, which is well suited for parametric studies.

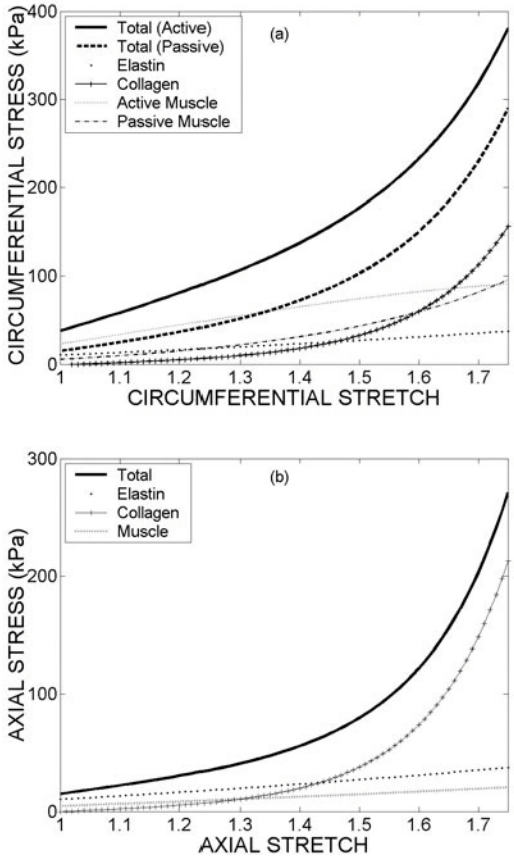

Figure 3. Stress-strain curves in the (a) θ-direction (λ_z = 1.50) and (b) z-direction (λ_θ = 1.50) for each constituent (elastin, collagen, and active and passive smooth muscle), and the mixture (active and passive). The total mixture response (solid curve) is similar to that predicted by equations (1)-(2) for a single constituent description. Note: $A^e/A = L^e/L = 0.85$, $A^c/A = 1.192$, $L^c/L = 1.125$, $A^m/A = L^m/L = 0.95$, T_B = 550 kPa, λ_M = 1.8, λ_o = 0.8, ϕ^f = 0.70, ϕ^e = 0.06, ϕ^c = 0.15, and ϕ^m = 0.09.

Consider a model carotid artery, in a 2-D rule-of-mixtures setting, having three primary structural constituents: elastin (e), collagen (c), and smooth muscle (m). Let the initial loaded radius and axial length (at P = 93 mmHg) be $a(0)$ = 2.25 mm and $\ell(0)$ = 7.5 cm; let $\phi^e(0)$ = 0.06, $\phi^c(0)$ = 0.15, and $\phi^m(0)$ = 0.09 (with water content ~0.70); and let the initial unloaded reference lengths be $A^e(0)$ =1.274 mm and $L^e(0)$ = 4.25 cm (thus, λ_i^e = 1.765) for elastin, $A^c(0)$ = 1.787 mm (λ_θ^c = 1.259) and $L^c(0)$ = 5.622 cm (λ_z^c = 1.334) for collagen, and $A^m(0)$ = 1.425 mm and $L^m(0)$ = 4.750 cm (λ_i^m = 1.579) for muscle, where $i = \theta$ or z. Individual constitutive relations for stress are listed in (42); these behaviors and the total 'mixture' behavior are illustrated in Figure 3. Although this model is based on illustrative material behaviors, not actual data, notice that many of the aforementioned characteristics are captured. Because of the 2-D setting, overall residual stress and material heterogeneities are not included. Nevertheless, the overall unloaded lengths are defined via that configuration in which residual constituent stresses balance to zero (e.g., elastin is tensile and collagen compressive in the absence of loads). The initial unloaded mixture reference is, $A(0)$ = 1.50 mm (for λ_θ=1.50) and $L(0)$ = 5.00 cm (λ_z=1.50), which were determined from equilibrium (equations (8) and (9)) with P = 0 and f_z = 0. Let us now compare biomechanical behaviors of native versus vessels lacking certain characteristics.

5.1. Engineering thickness

Given a = 2.25 mm, the predicted optimal thickness (see equation $(4)_2$) is h = 0.186 mm in a loaded configuration with P = 93 mmHg (~12.4 kPa) and σ_θ = 150 kPa; this corresponds to an unloaded thickness of H = 0.41 mm (assuming isochoric unloading, with A = 1.5 mm, ℓ = 7.5 cm, and L = 5.0 cm). Tissue-engineered vessels tend to be much thicker, however (e.g., H > 1 mm with A ~1.5 mm). Indeed such thickening is often encouraged to improve burst strengths and suture retention. Nevertheless, increasing vessel thickness yields a much higher structural stiffness and a much lower range of strains over physiological loading (Figure 4). For example, at λ_z = 1.5, the passive diameter is ~5.7 mm (λ_θ = 1.61) for H = 0.41 mm, but only ~3.5 mm (thus, λ_θ = 1.17) for H = 1.04 mm. It is important to note, therefore, that Niklason *et al*. (43) demonstrated that a 5% cyclic strain was necessary to achieve adequate collagen deposition and burst pressures (in a PGA-based construct); Seliktar *et al*. (44) also showed that significant cyclic strain was necessary to improve strength and construct contraction (in a collagen-gel based construct). Given the importance of cyclic strain *in vivo* as well as its apparent importance in tissue engineering, unless composed of more compliant constituents, a thicker-walled vessel may, in fact, exhibit a reduced ability to adapt functionally. Although the importance of burst strength and suture retention is duly noted, vessel wall thickening may not be the most advantageous parameter to achieve this design criterion.

5.2. Incorporating elastin

Next, consider a vessel with no elastin. Again let a=2.25 mm and ℓ=7.5 cm at 93 mmHg, but now let ϕ^c=0.1875 and ϕ^m=0.1125 (i.e., let collagen and muscle be in the same ratio as in the native vessel, and let the mass of structural constituents remain as 30%). Also, let A^c=1.787 mm (λ_θ^c=1.259) and L^c=5.622 cm (λ_z^c=1.334) and A^m=1.425 mm and L^m=4.750 cm (λ_i^m=1.579). For these conditions, the overall 2-D stress-free configuration is A=1.55 mm (for λ_θ=1.45) and L=5.34 cm (λ_z=1.40). The passive loading and stress-stretch curves reveal that such a vessel is stiffer both circumferentially (Figure 5) and axially (not shown). In particular, over the cardiac cycle, the elastin containing vessel would experience cyclic stretches from λ_θ=1.56 to 1.72 (16%), whereas the vessel with no elastin would experience λ_θ from 1.44 to 1.53 (9%). Again, this reduced level of cyclic strain could decrease adaptability.

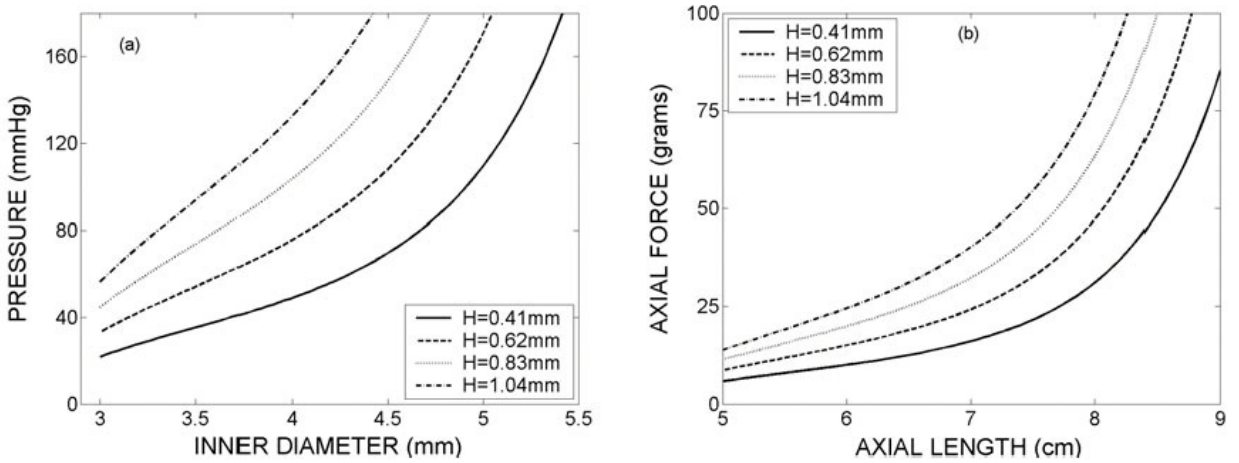

Figure 4. Simulations to illustrate possible effects of wall thickness on (a) pressure-diameter and (b) axial load-length curves. Note that A = 1.50 mm and L = 5.00 cm, $\phi^e = 0.06$, $\phi^c = 0.15$, $\phi^m = 0.09$, $\lambda_i^e = 1.765$ ($A^e = 1.274$ mm, and $L^e = 4.249$ cm), $\lambda_\theta^c = 1.259$ (thus $A^c = 1.787$ mm), $\lambda_z^c = 1.334$ ($L^c = 5.622$ cm), and $\lambda_i^m = 1.579$ ($A^m = 1.425$ mm, and $L^m = 4.750$ cm). Note, too, that H = 0.41 mm represents the 'optimal', unloaded wall thickness for this case.

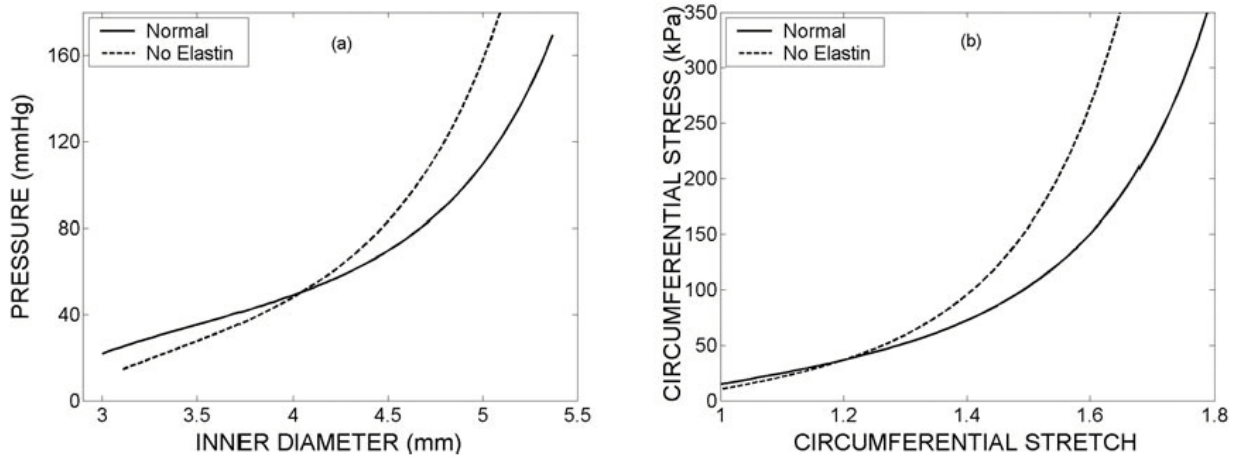

Figure 5. Simulations to illustrate possible effects of having no elastin. (a) pressure-diameter and (b) circumferential axial stress-stretch curves (at $\lambda_z = 1.5$) for a vessel containing no elastin (dashed) versus that of native elastin content. Note that a=2.25 mm and $\ell = 7.5$ cm at 93 mmHg, and $\lambda_i^e = 1.765$ (A^e =1.274 mm, and L^e =4.25 cm), $\lambda_\theta^c = 1.259$ (thus A^c =1.787 mm), $\lambda_z^c = 1.334$ (L^c =5.622 cm), and $\lambda_i^m = 1.579$ (A^m =1.425 mm, and L^m =4.750 cm). Note, too, that for the normal vessel ϕ^e =0.06, ϕ^c =0.15, ϕ^m =0.09, A=1.50 mm (λ_θ =1.50) and L = 5.00 cm (λ_z = 1.50); for the vessel with no elastin, $\phi^e = 0.00$, $\phi^c = 0.1875$, $\phi^m = 0.1125$ (i.e., the elastin is replaced with collagen and muscle in the same ratio as the native vessel), A = 1.55 mm ($\lambda_\theta = 1.45$) and L = 5.34 cm ($\lambda_z = 1.40$).

5.3. Engineering nonuniformity

A key advance in tissue-engineered arteries may turn out to be the incorporation of elastin as well as collagen and smooth muscle (cf. (45)). As noted above, however, we may also need to address the natural configuration of the elastin, not just its presence. Thus, consider model vessels, again with a = 2.25 mm and ℓ = 7.5 cm at 93 mmHg, $\phi^e = 0.06$, $\phi^c = 0.15$, and $\phi^m = 0.09$; moreover, let $\lambda_\theta^c = 1.259$ and $\lambda_z^c = 1.334$ and $\lambda_i^m = 1.579$ in the loaded configuration, but let the stretch ratios of elastin be $\lambda_i^e = 1.765$ (native), 1.50, or 1.20. Notice that, when elastin is present at stretch ratios higher than the other constituents, the vessel exhibits significant distension at low loads (Figure 6). Conversely, when the high pre-stretch of elastin is absent, this initial compliant behavior is reduced significantly, which reduces the mean and cyclic strains experienced by the smooth muscle cells. Thus, native vessels may exhibit significant distensibility at lower pressures not only because of the elastic properties of elastin, but also because of the separate natural configurations of the different constituents. That is, the difference in natural configurations can induce a type of local residual stress – the extended elastin can remain in tension when unloaded, which compresses the collagen and thereby increases its undulation and thus overall distensibility.

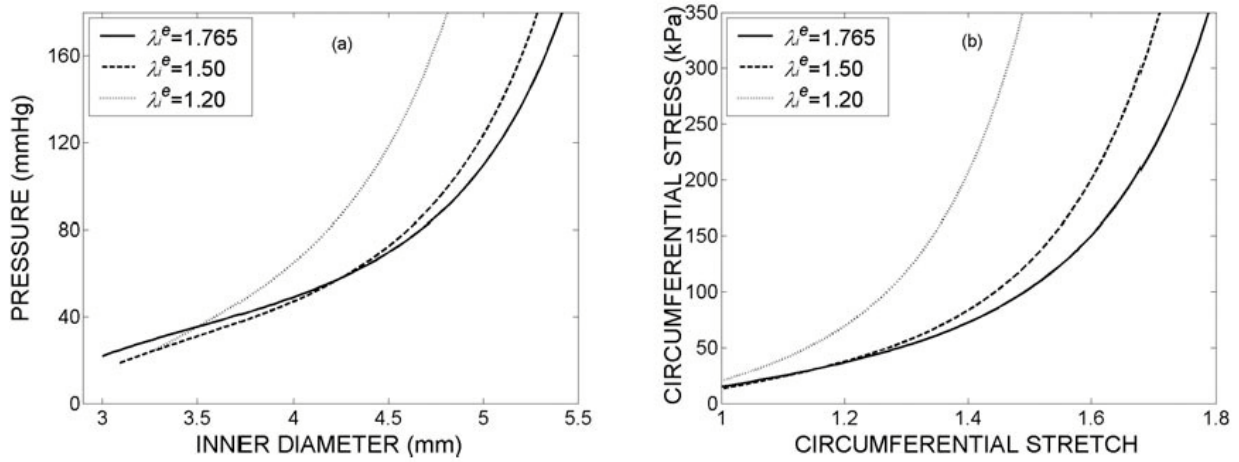

Figure 6. Simulations to illustrate possible effects of 'non-native' reference lengths of elastin. (a) pressure-diameter and (b) circumferential stress-stretch responses for various 'deposition stretches' for elastin. The model predicts an increased stiffness with a smaller deposition stretch, which results in part from the decreased initial compression (undulation) in the collagen as required by equilibrium in the unloaded state. Note that a = 2.25 mm and ℓ = 7.5 cm at 93 mmHg, ϕ^e = 0.06, ϕ^c = 0.15, ϕ^m = 0.09, λ_θ^c = 1.259 (thus A^c = 1.787 mm), λ_z^c = 1.334 (L^c = 5.622 cm), and λ_i^m = 1.579 (A^m = 1.425 mm, and L^m = 4.750 cm). Note, too, that for λ_i^e = 1.765 (A^e = 1.274 mm, and L^e = 4.25 cm), A = 1.50 mm and L = 5.00 cm; for λ_i^e = 1.765 (A^e = 1.500 mm, and L^e = 5.00 cm), A = 1.54 mm and L = 5.21 cm; and for λ_i^e = 1.765 (A^e = 1.875 mm, and L^e = 6.25 cm), A = 1.64 mm and L = 5.80 cm.

5.4. Engineering heterogeneity

Another potentially important criteria may be to build multi-layered vessels with morphological characteristics similar to native vessels (45). Here again, however, we may need to respect the configurations in which these layers are produced in normal development. Whereas the inner layers (intima, internal elastic lamima, etc.) are produced at 'small' diameters, the outer layers are produced and organized at larger diameters and lengths. Indeed, a low-pressure distensibility (endowed by the media) and high-pressure inextensibility (endowed by adventitia) support the idea that adventitial collagen experiences much less strain under normal physiologic loads. To illustrate, let us consider a model vessel consisting of two layers: a media-like layer with elastin, collagen, and smooth muscle and an adventitia-like layer composed mainly of collagen. Each layer is modeled as a membrane (i.e., radial variations in stretch are neglected within each layer) and the displacement of the outer wall of the inner membrane and the inner wall of the outer membrane are matched throughout loading. Furthermore, the transmural pressure across the inner membrane is (P – P_b) and that of the outer membrane is (P_b – 0), where P_b is the pressure at the interfacial boundary. Let the unloaded radius and axial length of the inner layer be A_1 = 1.5 mm and L_1 = 5.0 cm. Let the thickness of the vessel be H = 0.41 mm, with the thickness of the inner layer H_1 = 0.328 mm (= 0.80H) and the thickness of the outer layer H_2 = 0.082 mm (= 0.20H). Let the unloaded length of the outer layer be L_2 = 5.0 cm. Notice that, as the unloaded radius of the outer membrane is adjusted from A_2 = 1.60 to 2.40 (as in a shrink-fit problem), the vessel becomes much more distensible, with A_2 = 2.00 mm yielding a behavior similar to the native, single-layered vessel (Figure 7). Note that with A_2 = 1.828 mm, the vessel is residually stress-free in this two-layered model, whereas all other values impose a residual stress in the traction-free configuration (i.e., one layer is in compression and the other in tension in the absence of applied loads). Thus, for the tissue-engineered vessel, it not only may be necessary to incorporate a multi-layered construction, it may also be equally important to assemble each layer in the appropriate residually-stressed configuration (relative to the other layers) to mimic native biomechanical behavior.

6. CLOSURE

Although elastin was long thought to simply dominate low pressure behavior and endow vessels with significant elastic recoil, it is now clear that elastin plays many important structural, biological, and mechanical roles. Nevertheless, an intriguing and yet unanswered question in vascular mechanics relates to the differing distributions and organization of elastin throughout the vasculature. Elastin knockout models reveal that elastin is important developmentally in vessels from the aorta to arterioles, yet its role is accomplished via fundamentally different organizations (laminae versus diffuse) and mass fractions (e.g., 20-30% of wall in aorta but ~1% of wall in plantar artery). A key question for tissue engineering, therefore, is what mass fractions, distributions, and natural configurations are optimal for particular implants; indeed, the same is true with regard to the various types of collagen, proteoglycans, and even smooth muscle phenotypes. Much remains to be learned.

In closing, we hope that this paper stimulates some in biomechanics to study more deeply the mechanics

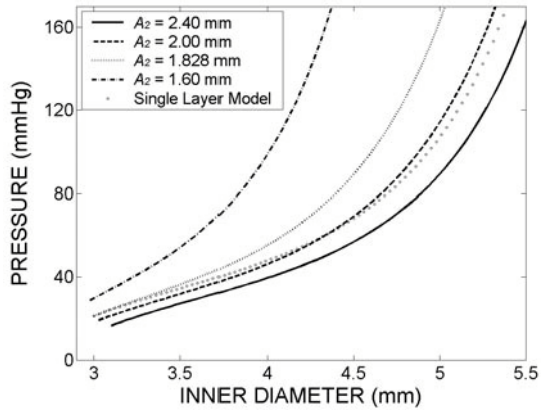

Figure 7. Pressure-diameter simulations using a two-layer membrane model (inner layer denoted by 1 and outer by 2) to illustrate the effect of heterogeneities for various unloaded radii for the outer layer: A_2 = 2.40, 2.00, 1.828 (no residual stress), and 1.60 mm. Note that A_1 = 1.5 mm, L_1 = 5.0 cm, H = 0.41 with H_1 = 0.328 (= 0.80H) and H_2=0.82 (= 0.20H), L_2 = 5.0 cm, ϕ_1^e = 0.06, ϕ_1^c = 0.15, ϕ_1^m =0.09, ϕ_2^e =0.00, ϕ_2^c =0.30, ϕ_2^m =0.00, $A^e/A_1 = A^e/A_2 = L^e/L_1 = L^e/L_2 = 0.85$, $A^c/A_1 = A^c/A_2 = 1.19$, $L^m/L_1 = L^m/L_2 = 1.12$, $A^m/A_1 = A^m/A_2 = L^m/L_1 = L^m/L_2 = 0.95$.

of arterial development - many clues for successful tissue engineering likely lie therein. Moreover, we hope that this paper stimulates some in arterial tissue engineering to consider more deeply the biomechanics, and in particular the potential use of time- and cost-efficient mathematical models for identifying classes of parameters that are most useful for study in the laboratory.

7. ACKNOWLEDGEMENTS

We thank Professor Shu Liu, Northwestern University, for inviting this contribution. We also acknowledge partial financial support via NSF grant BES-0084644 and NIH grant HL-64372 through the Bioengineering Research Partnerships Program.

8. REFERENCES

1. Weinberg, C. B. and E. Bell: A blood vessel model constructed from collagen and cultured vascular cells. *Science* 231, 397-400 (1986)

2. Nerem, R. M. and D. Seliktar: Vascular tissue engineering. *Annu Rev Biomed Eng* 3, 225-243 (2001)

3. Auger, F. A., G. Grenier, M. Remy-Zolghadri and L. Germain: A full spectrum of functional tissue-engineered blood vessels: from macroscopic to microscopic. In: Functional tissue engineering. Eds: Guilak F, Butler DL, Goldstein SA, Mooney DJ, Springer-Verlag, NY 347-359 (2003)

4. Mitchell, S. L. and L. E. Niklason: Requirements for growing tissue-engineered vascular grafts. *Cardiovasc Path* 12, 59-64 (2003)

5. Ku, D. N. and H-C. Han: Assessment of function in tissue-engineered vascular grafts. In: Functional tissue engineering. Eds: Guilak F, Butler DL, Goldstein SA, Mooney DJ, Springer-Verlag, NY, 258-267 (2003)

6. Humphrey, J. D: Cardiovascular solid mechanics: cells, tissues, organs. Springer-Verlag, NY (2002)

7. Holzapfel, G. A., T. C. Gasser and R. W. Ogden: A new constitutive framework for arterial wall mechanics and a comparative study of material models. In: Cardiovascular soft tissue mechanics. Eds: Cowin SC, Humphrey JD, Kluwer Academic Publishers, Boston (2000)

8. Chuong, C. J. and Y. C. Fung: On residual stress in arteries. *ASME J Biomech Engr* 108, 189-192 (1986)

9. Rachev, A. and K. Hayashi: Theoretical study of the effects of vascular smooth muscle contraction on strain and stress distributions in arteries. *Annls Biomed Engr* 27, 459-468 (1999)

10. Humphrey, J. D. and S. Na: Elastodynamics and arterial wall stress. *Annals Biomed Eng* 30, 509-523 (2002)

11. Davis, E. C: Elastic lamina growth in the developing mouse aorta. *J Histochem Cytochem* 43, 1115-1123 (1995)

12. Xu, J. and P. C. Brooks: Extracellular matrix in the regulation of angiogenesis. In: Assembly of the vasculature and its regulation. Ed: Tomanek RJ, Birkhauser, Boston (2002)

13. Clark, J. M. and S. Glagov: Structural integration of the arterial wall. *Lab Invest* 40, 587-602 (1979)

14. Zamir, M: Shear forces and blood vessel radii in the cardiovascular system. *J Gen Physiol* 69, 449-461 (1977)

15. Roach, M. R. and A. C. Burton: The reason for the shape of the distensibility curves of arteries. *Can J Biochem Physiol* 35, 681-690 (1957)

16. Alberts, B., A. Johnson, J. Lewis, M. Raff, K. Roberts and P. Walter: Molecular biology of the cell. 4th ed., Garland Science, New York (2002)

17. Dobrin, P. B., W. H. Baker and W. C. Gley: Elastolytic and collagenolytic studies of arteries. *Arch Surg* 119, 405-409 (1984)

18. Greenwald, S. E., J. E. Moore, A. Rachev, T. P. C. Kane and J-J. Meister: Experimental investigation of the distribution of residual strains in the artery wall. *ASME J Biomech Engr* 119, 438-444 (1997)

19. Zeller, P. J. and T. C. Skalak: Contribution of individual structural components in determining the zero-stress state in small arteries. *J Vasc Res* 35, 8-17 (1998)

20. Karnik, S. K., B. S. Brooke, A. Bayes-Genis, L. Sorensen, J. D. Wythe, R. S. Schwartz, M. T. Keating and

D. Y. Li: A critical role for elastin signaling in vascular morphogenesis and disease. *Development* 130, 411-423 (2003)

21. Li, D. Y., B. S. Brooke, E. C. Davis, R. P. Mecham, L. K. Sorensen, B. B. Boak, E. Eichwald and M. T. Keating: Elastin is an essential determinant of arterial morphogenesis. *Nature* 393, 276-280 (1998)

22. Dietz, H. C. and R. P. Mecham: Mouse models of genetic diseases resulting from mutations in elastic fiber proteins. *Matrix Biol* 19, 481-488 (2000)

23. Sugitani, H., H. Wachi, S. Tajima and Y. Seyama: Nitric oxide stimulates elastin expression in chick aortic muscle cells. *Biol Pharm Bull* 24, 461-464 (2001)

24. Wachi, H., H. Sugitani, S. Tajima and Y. Seyama: Endothelin-1 down-regulates expression of tropoelastin and lysly oxidase mRNA in cultured chick aortic smooth muscle cells. *J Health Science* 47, 525-532 (2001)

25. Krettek, A., G. K. Sukhova and P. Libby: Elastogenesis in human arterial disease. *Arterioscl Thromb Vasc Biol* 23, 582-587 (2003)

26. Matsumoto, T. and K. Hayashi: Mechanical and dimensional adaptation of rat aorta to hypertension. *ASME J Biomech Engr* 116, 278-283 (1994)

27. Fung, Y. C: Stress, strain, growth, and remodeling of living organisms. *ZAMP* 46, S469-485 (1995)

28. Taber, L.A: A model of aortic growth based on fluid shear and fiber stresses. *ASME J Biomech Engr* 120, 348-354 (1998)

29. Rachev, A: A model of arterial adaptation to alterations in blood flow. *J Elast* 61, 83-111 (2000)

30. Langille, B. L., M. P. Bendeck and F. W. Keeley: Adaptations of carotid arteries of young and mature rabbits to reduced carotid blood flow. *Am J Physiol* 256, H931-H939 (1989)

31. Kamiya, A. and T. Togawa: Adaptive regulation of wall shear stress to flow change in the canine carotid artery. *Am J Physiol* 239, H14-21 (1980)

32. Zarins, C. K., M. A. Zatina, D. P. Giddons, D. N. Ku and S. Glagov: Shear stress regulation of artery lumen diameter in experimental atherogenesis. *J Vasc Surg* 5, 413-420 (1987)

33. Lehman, R. M., G. K. Owens, N. F. Kassel and K. Hongo: Mechanism of enlargement of major cerebral collateral arteries in rabbits. *Stroke* 22, 499-504 (1991)

34. Unthank, J. L., S. W. Fath, H. M. Burkhart, S. C. Miller and M. C. Dalsing: Wall remodeling during luminal expansion of mesenteric arterial collaterals in the rat. *Circ Res* 79, 1015-1023 (1996)

35. Lu, X., J. B. Zhao, G. R. Wang, H. Gregersen and G. S. Kassab: Remodeling of the zero-stress state of femoral arteries in response to flow overload. *Am J Physiol* 280, H1547-1559 (2001)

36. Fung, Y. C. and S. Q. Liu: Change of residual strains in arteriesdue to hypertrophy caused by aortic constriction. *Cir Res* 65, 1340-1349 (1989)

37. Jackson, Z. S., A. I. Gotlieb and L. Langille: Wall tissue remodeling regulates longitudinal tension in arteries. *Circ Res* 90, 918-925 (2002)

38. Han, H-C., D. N. Ku and R. P. Vito: Arterial wall adaptation under elevated longitudinal stretch in organ culture. *Annals Biomed Eng* 31, 403-411 (2003)

39. Clerin, V., J. W. Nichol, M. Petko, R. J. Myung, J. W. Gaynor and K. J. Gooch: Tissue engineering of arteries by direct remodeling of intact arterial segments. *Tissue Eng* 9, 461-472 (2003)

40. Rodriguez, E. K., A. Hoger and A. D. McCulloch: Stress-dependent finite growth in soft elastic tissues. *J Biomech* 27, 455-467 (1994)

41. Humphrey, J. D. and K. R. Rajagopal: A constrained mixture model for arterial adaptations to a sustained step change in blood flow. *Biomech Model Mechanobiol* 2, 109-126 (2003)

42. Gleason, R. L., L. A. Taber and J. D. Humphrey: A 2-D model of flow-induced alterations in the geometry, structure, and properties of carotid arteries. *ASME J Biomech Eng* (in press) (2004)

43. Niklason, L. E., J. Gao, W. M. Abbott, K. Hirschi, S. Houser, R. Marini and R. Langer: Functional arteries grown *in vitro*. *Science* 284, 489-493 (1999)

44. Seliktar, D., R. A. Black, R. P. Vito and R. M. Nerem: Dynamic mechanical conditioning of collagen-gel blood vessel constructs induces remodeling *in vitro*. *Annals Biomed Eng* 28, 351-362 (2000)

45. L'Heureux, N., S. Paquet, R. Labbe, L. Germain and F. A. Auger: A completely biological tissue-engineered human blood vessel. *FASEB J* 12, 47-56 (1998)

Footnotes: [1] Holzapfel *et al*. (7) show that this relation is convex if the material parameters are chosen appropriately. [2] That is, large deformations, nonlinear elastic behavior, and pressurization of a cylindrical structure tend to induce strong transmural gradients in stress or strain. [3] Although we consider only a 2-D (mean) state of stress, the wall is allowed to have a finite thickness h.

Key Words: Vascular tissue engineering, Vascular mechanics, Growth and remodeling, Stress, Elastin, Review

Send correspondence to: Dr Jay D. Humphrey, Department of Biomedical Engineering, Texas, A&M University, MS-3120, 233 Zachry Engineering Center, College Station, TX 77843-3120, Tel:979-845-5558, Fax: 979-845-4450, E-mail: jhumphrey@tamu.edu